



# Chaotic dynamics and the role of covariance inflation for reduced rank Kalman filters with model error

Colin Grudzien<sup>1</sup>, Alberto Carrassi<sup>1</sup>, and Marc Bocquet<sup>2</sup>

<sup>1</sup>Nansen Environmental and Remote Sensing Center, Bergen, Norway

<sup>2</sup>CEREA, joint laboratory École des Ponts ParisTech and EDF R&D, Université Paris-Est, Champs-sur-Marne, France

*Correspondence to:* Colin Grudzien, Colin.Grudzien@nersc.no

**Abstract.** The ensemble Kalman filter and its variants have shown to be robust for data assimilation in high dimensional geophysical models, with localization, using ensembles of extremely small size relative to the model dimension. A reduced rank representation of the estimated covariance, however, leaves a large dimensional complementary subspace unfiltered. Utilizing the dynamical properties of the filtration for the backward Lyapunov vectors, this paper explores a previously unexplained mechanism, describing the intrinsic role of covariance inflation in reduced rank, ensemble based Kalman filters. Our derivation of the forecast error evolution describes the dynamic upwelling of the unfiltered error from outside of the span of the anomalies into the filtered subspace. Analytical results for linear systems explicitly describe the mechanism for the upwelling, and the associated recursive Riccati equation for the forecast error, while nonlinear approximations are explored numerically.

## 1 Introduction

It is well understood that in chaotic physical systems, dynamical instability is among the leading drivers of forecast uncertainty (Trevisan and Palatella, 2011a; Vannitsem, 2017). Recent mathematical and numerical results have, furthermore, established a rigorous framework for understanding the relationship between dynamical instability, in terms of the non-negative Lyapunov exponents, and the asymptotic properties of the uncertainty in ensemble based data assimilation techniques: in perfect models, with weakly-nonlinear error growth, it was shown that the ensemble of anomalies projects strongly on the span of the unstable-neutral backward Lyapunov vectors (Sakov and Oke, 2008; Carrassi et al., 2009; Ng et al., 2011; González-Tokman and Hunt, 2013; Bocquet and Carrassi, 2017), and that the divergence of the ensemble Kalman filter depends significantly upon whether error in this space is sufficiently observed and corrected.

Inspired by the Assimilation in the Unstable Subspace (AUS) methodology of Anna Trevisan and her collaborators (Trevisan and Ubaldi, 2004; Carrassi et al., 2007, 2008; Trevisan et al., 2010; Trevisan and Palatella, 2011b; Palatella et al., 2013; Palatella and Trevisan, 2015), recent mathematical results have rigorously validated the underlying hypothesis of AUS: for perfect, linear models, the uncertainty of the Kalman filter asymptotically collapses to the span of the backward Lyapunov vectors with non-negative exponents (Gurumoorthy et al., 2017). Furthermore, if a sub-optimal filter has an estimated covariance initialized only in these modes, and the unstable-neutral subspace is uniformly, completely observed, the sub-optimal filter becomes asymptotically equivalent to the optimal Kalman filter (Bocquet et al., 2017). This phenomenon has, furthermore, been



generalized as a criterion for the exponential stability of continuous time filters, in perfect models, in terms of the *detectability* of the unstable-neutral subspace (Frank and Zhuk, 2017).

The above mathematical results demonstrate how the stable dynamics in perfect models dissipate forecast errors, in sequential filters, such that a reduced rank representation of the error covariance, in the unstable-neutral subspace alone, suffices to 5 control error growth. This behavior, similarly understood in the smoothing problem (Pires et al., 1996; Trevisan et al., 2010), is now also mathematically verified for the linear Kalman smoother, and its nonlinear ensemble formulation is shown numerically to exhibit the same behavior, in a weakly-nonlinear regime for error dynamics (Bocquet and Carrassi, 2017).

The work of Grudzien et al. (2017) extends the mathematical framework for AUS, so far established for perfect models, to the presence of additive model errors with additional qualifications: in the absence of observations, model dynamics alone 10 are still sufficient to uniformly bound the errors in the span of the stable backward Lyapunov vectors. However, the uniform bound may be impractically large due to the excitation of model errors by the transient instabilities in stable directions. While uncertainty is *asymptotically* dissipated by the stable dynamics, the reintroduction of uncertainty from model error significantly differentiates imperfect models. Newly injected errors are subject to the growth rates of the local (in time) Lyapunov exponents, and stable Lyapunov exponents of sufficiently high variance may experience transient periods of growth. Therefore, strategies 15 for representing the forecast error with a reduced rank ensemble must be adapted for imperfect models to account for a residual error in the span of the stable, backward Lyapunov vectors which never vanishes and, moreover, may go through transient periods of growth. As a consequence, confining the error description within a reduced rank Kalman filter to only the unstable-neutral subspace does not suffice when model error is present and suggests that one must include additional, asymptotically stable, modes.

20 In this work we show, furthermore, that such an increase of the ensemble span does not automatically render the filter optimal: one may also need to account for the injection of error from unfiltered directions into the ensemble span. In particular, when a reduced rank, ensemble based Kalman gain is used to correct the forecast errors, the dynamics induce error propagation which transmits uncertainty from the uncorrected, complementary subspace into the ensemble span. In this study, the propagation of error in the linear Kalman filter, written in a basis of backward Lyapunov vectors, will reveal the leading order 25 evolution of the unfiltered uncertainty. Although the evolution is derived for linear models, the mechanism for error propagation can be considered a generic feature of reduced rank ensemble Kalman filters: under the condition that error evolution is weakly-nonlinear, the ensemble span will align with the span of the leading backward Lyapunov vectors — therefore the error decomposition in the basis of backward Lyapunov vectors will be valid for the ensemble Kalman filter.

This paper is structured as follows: section 2.1 concerns essential results from the theory of Lyapunov vectors which will 30 be used throughout; sections 2.2 and 2.3 describe the basic framework for the Kalman filter, and will motivate our subsequent results; section 3 contains our main analytical result, i.e., the derivation of the evolution of forecast error under a sub-optimal filter in a basis of backward Lyapunov vectors; finally, section 4 will use numerics to qualitatively explore the ideal linear recursion for the forecast error of the sub-optimal filter, and its approximation in nonlinear models. Conclusions are drawn in section 5



## 2 Preliminaries

We begin by introducing our notation and the problem formulation.

### 2.1 Lyapunov vectors

Throughout the entire text, the conventional notation  $k = 0, 1, 2, \dots$  is adopted to indicate that the quantity is defined at time  $t_k$ .

5 Let  $\mathbf{z}_{k-1} \in \mathbb{R}^n$  be an arbitrary vector, the matrix propagator of the forward model from  $t_{k-1}$  to  $t_k$  is given by  $\mathbf{M}_k$ , such that  $\mathbf{z}_k = \mathbf{M}_k \mathbf{z}_{k-1}$ . We denote the operator taking the system state from an arbitrary time  $t_l$  to  $t_k$  as  $\mathbf{M}_{k:l} \triangleq \mathbf{M}_k \mathbf{M}_{k-1} \dots \mathbf{M}_{l+1}$ , with the symbol  $\triangleq$  used to signify that the expression is a definition. We will denote  $\mathbf{M}_{k:k} \triangleq \mathbf{I}_n$ , where  $\mathbf{I}_n$  is the identity matrix (of size  $n \times n$  in this case). At all times we assume  $\mathbf{M}_k$  to be non-singular and to be uniformly bounded in  $k$ .

Although much of the derivations that follow are done for linear dynamics, we are ultimately concerned with nonlinear systems — therefore, we will assume that Oseledec's theorem holds, even for linear model propagators. In general, this is a non-trivial assumption, but one which can be considered generic for the tangent-linear model of nonlinear systems (Barreira and Pesin, 2002, see the Multiplicative Ergodic theorem, Theorem 2.1.2). The backward Lyapunov vectors can be defined by a choice of an orthonormal eigenbasis for the far-past operator (Kuptsov and Parlitz, 2012).

15 **Definition 1.** Define the matrix  $\mathbf{E}_k$  to be the orthogonal matrix whose  $i$ th column is the  $i$ th **backward Lyapunov vector (BLV)** at time  $k$ , corresponding to the Lyapunov exponent  $\lambda_i$ .

We order the Lyapunov exponents

$$\lambda_1 \geq \dots \geq \lambda_{n_0} \geq 0 > \lambda_{n_0+1} \geq \dots \geq \lambda_n, \quad (1)$$

such that the unstable-neutral subspace is defined to be of dimension  $n_0$  and the model state dimension is  $n$ . Note, we do not assume that the Lyapunov exponents are distinct.

20 We will utilize the invariance of the BLVs under the recursive QR algorithm of Benettin et al. (1980) and Shimada and Nagashima (1979).

**Lemma 1.** There is an  $n \times n$  upper triangular matrix  $\mathbf{U}_k$ , such that the (tangent-linear) model propagator satisfies

$$\mathbf{M}_k = \mathbf{E}_k \mathbf{U}_k \mathbf{E}_{k-1}^T \quad (2)$$

The diagonal elements of  $\mathbf{U}_k$ , denoted  $U_k^i$ , define the local Lyapunov exponents.

25 *Proof.* Equation (2) follows from Eq. (31) of Kuptsov and Parlitz (2012) and is a simple consequence of the invariance of the BLVs under the recursive QR decomposition (Grudzien et al., 2017).  $\square$

The decomposition in Eq. (2) represents a change of basis of the model space into the upper triangular dynamics of the backward Lyapunov filtration (Legras and Vautard, 1996). In particular,  $\mathbf{E}_{k-1}^T$  takes the model state into the orthogonal projection



coefficients in the basis of BLVs at time  $k - 1$ . We will denote the projection coefficients of an arbitrary vector  $\mathbf{z}_k$  into a basis of BLVs with a “hat”, i.e.  $\mathbf{E}_k^T \mathbf{z}_k \triangleq \hat{\mathbf{z}}_k$ . Using the orthogonality of the matrix  $\mathbf{E}_k$ , the invariant dynamics in the BLVs is written

$$\hat{\mathbf{z}}_k = \mathbf{U}_k \hat{\mathbf{z}}_{k-1} \Leftrightarrow \mathbf{z}_k = \mathbf{M}_k \mathbf{z}_{k-1}. \quad (3)$$

The operator  $\mathbf{U}_k$  thus describes the invariant, upper triangular dynamics, transferring the model state into its forward representation in the BLVs at time  $k$ .

## 2.2 The Kalman filter

We seek to estimate the distribution of a Gaussian random variable evolved via a linear Markov model with additive white noise,

$$\mathbf{x}_k = \mathbf{M}_k \mathbf{x}_{k-1} + \mathbf{w}_k, \quad (4)$$

and with observations given in the form

$$\mathbf{y}_k = \mathbf{H}_k \mathbf{x}_k + \mathbf{v}_k. \quad (5)$$

The forecast mean,  $\mathbf{x}_k^b$ , is propagated from the last posterior mean,  $\mathbf{x}_{k-1}^a$  by the deterministic component of Eq. 4, i.e.,

$$\mathbf{x}_k^b = \mathbf{M}_k \mathbf{x}_{k-1}^a. \quad (6)$$

The model variables  $\mathbf{x}_k \in \mathbb{R}^n$  and observational variables  $\mathbf{y}_k \in \mathbb{R}^d$ , are related via the linear observation operator  $\mathbf{H}_k : \mathbb{R}^n \mapsto \mathbb{R}^d$ . Model and observation noise,  $\mathbf{w}_k$  and  $\mathbf{v}_k$ , are assumed mutually independent, unbiased, Gaussian white sequences such that

$$\mathbb{E}[\mathbf{v}_k \mathbf{v}_l^T] = \delta_{k,l} \mathbf{R}_k \quad \text{and} \quad \mathbb{E}[\mathbf{w}_k \mathbf{w}_l^T] = \delta_{k,l} \mathbf{Q}_k, \quad (7)$$

where  $\mathbb{E}$  is the expectation,  $\mathbf{R}_k \in \mathbb{R}^{d \times d}$  is the observation error covariance matrix at time  $t_k$ , and  $\mathbf{Q}_k \in \mathbb{R}^{n \times n}$  stands for the model error covariance matrix. The error covariance matrix  $\mathbf{R}_k$  can be assumed invertible without losing generality. To avoid pathologies, we assume that the model error and the observational error covariance matrices are uniformly bounded. For  $1 \leq t < s \leq n$ , and given a matrix  $\mathbf{A} \in \mathbb{R}^{n \times n}$ , we define  $\mathbf{A}^{t:s} \in \mathbb{R}^{n \times s-t+1}$  to be the matrix composed (inclusively) of columns  $s$  through  $t$  of  $\mathbf{A}$ .

**Definition 2.** *The forecast error is defined as the difference of the mean state estimated by the filter and the unknown random state, i.e.,*

$$\epsilon_k \triangleq \mathbf{x}_k^b - \mathbf{x}_k. \quad (8)$$

*The innovation is the measured difference between the forecast and observation,*

$$\delta_k \triangleq \mathbf{y}_k - \mathbf{H}_k \mathbf{x}_k = \mathbf{H}_k \epsilon_k - \mathbf{v}_k. \quad (9)$$



We define the **true forecast error covariance** at time  $k$  to be

$$\mathbf{B}_k \triangleq \mathbb{E} [\boldsymbol{\epsilon}_k \boldsymbol{\epsilon}_k^T]. \quad (10)$$

On the other hand, suppose some filter, yet to be identified, is used to estimate the forecast mean and error covariance — the **estimated forecast error covariance** will be denoted  $\mathbf{P}_k$ , defined according to the chosen estimation algorithm.

5 Suppose that  $\mathbf{K}_k \in \mathbb{R}^{n \times d}$  is some estimator which takes the forecast state to the analysis state. In the case of the *ideal* Kalman filter, where the true forecast error covariances are computed exactly,  $\mathbf{K}_k$  will be defined

$$\begin{aligned} \mathbf{K}_k &\triangleq \mathbf{P}_k \mathbf{H}_k^T (\mathbf{H}_k \mathbf{P}_k \mathbf{H}_k^T + \mathbf{R}_k)^{-1} \\ &= \mathbf{B}_k \mathbf{H}_k^T (\mathbf{H}_k \mathbf{B}_k \mathbf{H}_k^T + \mathbf{R}_k)^{-1} \end{aligned} \quad (11)$$

In this text, we will vary the choice of the analysis update operator  $\mathbf{K}_k$ , but the functional form of the recursion for the analysis 10 update of the mean will be unchanged and defined as

$$\begin{aligned} \mathbf{x}_k^a &\triangleq \mathbf{x}_k^b + \mathbf{K}_k (\mathbf{y}_k - \mathbf{H}_k \mathbf{x}_k^b) \\ &= \mathbf{x}_k^b - \mathbf{K}_k \mathbf{H}_k \boldsymbol{\epsilon}_k + \mathbf{K}_k \mathbf{v}_k. \end{aligned} \quad (12)$$

Therefore, for any estimator, the forecast mean can be derived recursively from Eq. (6) and Eq. (12) as

$$\mathbf{x}_{k+1}^b \triangleq \mathbf{M}_{k+1} (\mathbf{x}_k^b - \mathbf{K}_k \mathbf{H}_k \boldsymbol{\epsilon}_k + \mathbf{K}_k \mathbf{v}_k) \quad (13)$$

15 where  $\mathbf{K}_k$  is some choice for the gain. The recursion on the forecast error can be derived equal to

$$\boldsymbol{\epsilon}_{k+1} \triangleq \mathbf{M}_{k+1} [(\mathbf{I}_n - \mathbf{K}_k \mathbf{H}_k) \boldsymbol{\epsilon}_k + \mathbf{K}_k \mathbf{v}_k] - \mathbf{w}_{k+1}, \quad (14)$$

though  $\boldsymbol{\epsilon}_k$ ,  $\mathbf{v}_k$  and  $\mathbf{w}_{k+1}$  are assumed to be unknown.

### 2.3 Rank deficiency in the Kalman filter

In an ideal linear model, with known, Gaussian observational and model error distributions, the estimated and true error 20 covariances of the KF are equal: the posterior error distribution for the state is Gaussian, and the KF completely describes the posterior through its recursive equations for the estimated mean and covariance. However, it is often the case that the recursion for the posterior error distribution is approximated with a reduced rank surrogate in which the estimated covariance,  $\mathbf{P}_k$ , and resulting true error covariance,  $\mathbf{B}_k$ , may not be equal (Chandrasekar et al., 2008). This mis-match between the approximated and true forecast error covariance, and the resultant sub-optimal analysis update, can lead to systematic underestimation of the 25 true forecast error and filter divergence.

Nonetheless, it is possible in an ideal setting to analytically describe the error statistics of a reduced rank Bayesian filter — to illustrate this, assume we have a linear model with known Gaussian error distributions. Suppose we apply the analysis



update in a reduced rank set of BLVs, as has been done in EKF-AUS (Trevisan and Palatella, 2011b). Suppose, furthermore, the true error covariance,  $\mathbf{B}_k$ , is known. Then the gain

$$\mathbf{K}_k \triangleq \mathbf{E}_k^{1:n_0} (\mathbf{E}_k^{1:n_0})^T \mathbf{B}_k \mathbf{E}_k^{1:n_0} (\mathbf{E}_k^{1:n_0})^T \mathbf{H}_k^T \times \\ \left[ \mathbf{H}_k \mathbf{E}_k^{1:n_0} (\mathbf{E}_k^{1:n_0})^T \mathbf{B}_k \mathbf{E}_k^{1:n_0} (\mathbf{E}_k^{1:n_0})^T \mathbf{H}_k^T + \mathbf{R}_k \right]^{-1} \quad (15)$$

5 yields the *exact Bayesian update with respect to a subset of the anomaly variables*, defined by the span of the leading  $n_0$  BLVs. We may use Eq. (14) to derive the analytical recursion for the covariance of the true forecast error under the sub-optimal analysis operator in Eq. (15). As in the ideal KF, this will describe the ideal forecast error recursion with respect to a rank deficient estimator — the **rank deficiency (or reduced rank)** is defined by the restriction of the Bayesian update to a low dimensional subspace.

10 The significance of deriving an analytical recursion for the forecast error under the sub-optimal estimator in Eq. (15) is as follows. The analysis operator in Eq. (15) is characteristic of the generic gain for the ensemble Kalman filter (**EnKF**) in large, geophysical models: the ensemble based gain applies its update with respect to the subspace defined by the span of the ensemble of anomalies, which is typically of low rank and aligns with the span of the leading BLVs (Bocquet and Carrassi, 2017). The EnKF is, therefore, a Monte Carlo estimate of the true error statistics resulting from a rank deficient analysis update

15 as in Eq. (15). The *ideal error distribution* that the EnKF samples is thus characterized by the recursion derived for the error under the rank deficient Bayesian estimator. This is the motivation of section 3, where we will define a sub-optimal analysis gain, which operates within the span of an arbitrary number of the leading BLVs, and derive the resulting true forecast error covariance.

### 3 Filtering in the backward Lyapunov basis vectors

20 Consider the forecast error recursion for the linear KF in Eq. (14). As we are motivated by reduced rank ensemble covariances, suppose  $\mathbf{K}_k$  is defined as a sub-optimal gain which corrects only the leading  $r$  BLVs, with  $r < n$ . We denote the filtered subspace by the column span of the vectors  $\mathbf{E}_k^f \triangleq \mathbf{E}_k^{1:r}$  and the unfiltered subspace  $\mathbf{E}_k^u \triangleq \mathbf{E}_k^{r+1:n}$  for all  $k$ . The projection coefficients of a vector  $\mathbf{z} \in \mathbb{R}^n$  into the filtered and unfiltered subspace will be denoted  $\hat{\mathbf{z}}^f \triangleq (\mathbf{E}_k^f)^T \mathbf{z}$  and  $\hat{\mathbf{z}}^u \triangleq (\mathbf{E}_k^u)^T \mathbf{z}$ , respectively. We can thus decompose the forecast error into its orthogonal projections in the filtered and unfiltered subspaces

25 as

$$\epsilon_k \triangleq \mathbf{E}_k^f \hat{\epsilon}_k^f + \mathbf{E}_k^u \hat{\epsilon}_k^u. \quad (16)$$

For  $i, j \in \{f, u\}$ , we write the sub-covariances in the basis defined by  $\mathbf{E}_k$  as

$$\hat{\mathbf{B}}_k^{ij} \triangleq \mathbb{E} \left[ \hat{\epsilon}_k^i \left( \hat{\epsilon}_k^j \right)^T \right]. \quad (17)$$



such that the true forecast error covariance is given

$$\mathbf{B}_k \equiv \mathbf{E}_k \begin{pmatrix} \widehat{\mathbf{B}}_k^{\text{ff}} & \widehat{\mathbf{B}}_k^{\text{fu}} \\ \widehat{\mathbf{B}}_k^{\text{uf}} & \widehat{\mathbf{B}}_k^{\text{uu}} \end{pmatrix} \mathbf{E}_k^T, \quad (18)$$

where  $\widehat{\mathbf{B}}_k^{\text{ff}}$  and  $\widehat{\mathbf{B}}_k^{\text{uu}}$  are symmetric. We will write  $\mathbf{U}_k$  as a block matrix as

$$\mathbf{U}_k \triangleq \begin{pmatrix} \mathbf{U}_k^{\text{ff}} & \mathbf{U}_k^{\text{fu}} \\ \mathbf{0}_{n-r \times r} & \mathbf{U}_k^{\text{uu}} \end{pmatrix}. \quad (19)$$

5 For an arbitrary filtered subspace, the sub-optimal gain  $\mathbf{K}_k$ , which corrects only the span of  $\mathbf{E}_k^{\text{f}}$ , is defined by

$$\mathbf{K}_k \triangleq \mathbf{E}_k^{\text{f}} \widehat{\mathbf{K}}_k, \quad (20)$$

$$\widehat{\mathbf{K}}_k \triangleq \mathbf{B}_k^{\text{ff}} (\mathbf{E}_k^{\text{f}})^T \mathbf{H}_k^T \left[ \mathbf{H}_k \mathbf{E}_k^{\text{f}} \mathbf{B}_k^{\text{ff}} (\mathbf{E}_k^{\text{f}})^T \mathbf{H}_k^T + \mathbf{R}_k \right]^{-1},$$

Where  $\widehat{\mathbf{K}}_k$  represents the projection coefficients of the sub-optimal gain into the filtered variables.

For every  $k \geq 1$ , we decompose the model error covariance into the basis of filtered and unfiltered BLVs as

$$10 \quad \mathbf{Q}_k \triangleq \mathbf{E}_k \begin{pmatrix} \widehat{\mathbf{Q}}_k^{\text{ff}} & \widehat{\mathbf{Q}}_k^{\text{fu}} \\ \widehat{\mathbf{Q}}_k^{\text{uf}} & \widehat{\mathbf{Q}}_k^{\text{uu}} \end{pmatrix} \mathbf{E}_k^T \quad (21)$$

where  $\widehat{\mathbf{Q}}_k^{\text{ff}}$  and  $\widehat{\mathbf{Q}}_k^{\text{uu}}$  are symmetric matrices.

With the above notation, and using Eq. (2), the evolution of the true forecast error under the sub-optimal gain is derived from Eq. (14) as

$$15 \quad \begin{aligned} \epsilon_{k+1} &= \mathbf{M}_{k+1} \left( \mathbf{I}_n - \mathbf{E}_k^{\text{f}} \widehat{\mathbf{K}}_k \mathbf{H}_k \right) \epsilon_k + \mathbf{M}_{k+1} \mathbf{E}_k^{\text{f}} \widehat{\mathbf{K}}_k \mathbf{v}_k - \mathbf{w}_{k+1} \\ &= \left( \mathbf{E}_{k+1} \mathbf{U}_{k+1} \mathbf{E}_k^T - \mathbf{E}_{k+1} \mathbf{U}_{k+1} \mathbf{I}_{n \times r} \widehat{\mathbf{K}}_k \mathbf{H}_k \right) \epsilon_k + \mathbf{E}_{k+1} \mathbf{U}_{k+1} \mathbf{I}_{n \times r} \widehat{\mathbf{K}}_k \mathbf{v}_k - \mathbf{w}_{k+1}. \end{aligned} \quad (22)$$

Equation (22) describes the evolution of the true forecast error in the sub-optimal filter, and suggests, as in Eq. (3), how we may write the error evolution into the invariant upper triangular dynamics of the BLVs. Specifically, we consider the projections of the forecast error into the filtered and unfiltered subspaces under the forecast-analysis update cycle in Eq. (22). Computing the evolution of  $\widehat{\epsilon}_k^{\text{f}}$  and  $\widehat{\epsilon}_k^{\text{u}}$ , we may derive the exact recursion for  $\widehat{\mathbf{B}}_k^{\text{ff}}$ , i.e., the *exact* forecast uncertainty in the filtered subspace, 20 under a gain which operates in the span of the leading  $r$  BLVs.

### 3.1 Evolution of unfiltered error

Here we will derive the evolution of error in the unfiltered subspace, and verify that it evolves according to the free evolution. Notice first the following relation,

$$(\mathbf{E}_{k+1}^{\text{u}})^T \mathbf{E}_{k+1} \mathbf{U}_{k+1} \mathbf{I}_{n \times r} = \mathbf{0}_{n-r \times r}, \quad (23)$$



due to the fact that  $\mathbf{E}_{k+1}$  is an orthogonal matrix and, therefore, that the above product is equal to the lower left block of  $\mathbf{U}_{k+1}$ , which is upper triangular. With substitution of Eq. (16) into Eq. (22) for  $\boldsymbol{\epsilon}_k$ , multiplying on the left by  $(\mathbf{E}_k^u)^T$  to move into the unfiltered subspace, and by utilizing Eq. (23) to cancel the error in the filtered space, we find

$$5 \quad \hat{\boldsymbol{\epsilon}}_{k+1}^u = (\mathbf{E}_{k+1}^u)^T \mathbf{E}_{k+1} \mathbf{U}_{k+1} \mathbf{E}_k^T (\mathbf{E}_k^f \hat{\boldsymbol{\epsilon}}_k^f + \mathbf{E}_k^u \hat{\boldsymbol{\epsilon}}_k^u) - (\mathbf{E}_{k+1}^u)^T \mathbf{w}_{k+1} \quad (24)$$

$$= \mathbf{U}_{k+1}^{uu} \hat{\boldsymbol{\epsilon}}_k^u - \hat{\mathbf{w}}_{k+1}^u. \quad (25)$$

Equation (25) demonstrates that the evolution of the error in the unfiltered subspace follows exactly the free forecast evolution. The unfiltered error can be induced as mean zero, with covariance at time  $k$  equal to

$$\hat{\mathbf{B}}_k^{uu} = \mathbf{U}_{k:0}^{uu} \hat{\mathbf{B}}_0^{uu} (\mathbf{U}_{k:0}^{uu})^T + \sum_{l=1}^k \mathbf{U}_{k:l}^{uu} \hat{\mathbf{Q}}_l^{uu} (\mathbf{U}_{k:l}^{uu})^T. \quad (26)$$

10 The initial uncertainty in the unfiltered subspace evolves as  $\mathbf{U}_{k:0}^{uu} \hat{\mathbf{B}}_0^{uu} (\mathbf{U}_{k:0}^{uu})^T$  and thus, when  $r > n_0$ , vanishes exponentially. This implies that asymptotic unfiltered error is independent of the initialization, similar to the results of Bocquet et al. (2017). The remaining sum in Eq. (26) represents the contribution to the current forecast uncertainty from model error at all subsequent times, propagated under the upper triangular evolution in the BLVs. Therefore, while the initial error is forgotten, the asymptotic error in the reduced rank filter here explicitly depends on the dimension of the unfiltered subspace and the local variability of  
 15 the stable BLVs therein.

The error in the  $i$  th BLV in Eq. (26) is given by the invariant evolution of perturbations, formerly studied by Grudzien et al. (2017): when the filtered subspace dimension is of dimension  $r \geq n_0$ , we can recursively, and stably, compute the unfiltered uncertainty via

$$\hat{\mathbf{B}}_{k+1}^{uu} = \hat{\mathbf{Q}}_{k+1}^{uu} + \mathbf{U}_{k+1}^{uu} \hat{\mathbf{B}}_k^{uu} (\mathbf{U}_{k+1}^{uu})^T. \quad (27)$$

20 When  $r < n_0$ , we see explicitly that the filter will diverge as a consequence of leaving an unstable direction unfiltered.

### 3.2 Evolution of filtered error

While the evolution of the unfiltered error in Eq. (26) is a simple extension of the results from Grudzien et al. (2017), that work did not explicitly consider the evolution of error in a reduced rank filter — we now consider the evolution of the projection of the forecast error into the filtered space, with respect to the reduced rank gain. From Eq. (22) we derive

$$25 \quad \hat{\boldsymbol{\epsilon}}_{k+1}^f = (\mathbf{E}_{k+1}^f)^T \mathbf{E}_{k+1} \mathbf{U}_{k+1} \mathbf{E}_k^T (\mathbf{E}_k^f \hat{\boldsymbol{\epsilon}}_k^f + \mathbf{E}_k^u \hat{\boldsymbol{\epsilon}}_k^u) \\ - (\mathbf{E}_{k+1}^f)^T \mathbf{E}_{k+1} \mathbf{U}_{k+1} \mathbf{I}_{n \times r} \hat{\mathbf{K}}_k \mathbf{H}_k (\mathbf{E}_k^f \hat{\boldsymbol{\epsilon}}_k^f + \mathbf{E}_k^u \hat{\boldsymbol{\epsilon}}_k^u) \\ + (\mathbf{E}_{k+1}^f)^T (\mathbf{E}_{k+1} \mathbf{U}_{k+1} \mathbf{I}_{n \times r} \hat{\mathbf{K}}_k \mathbf{v}_k - \mathbf{w}_{k+1}). \quad (28)$$



Similar to Eq. (23), we see that the terms

$$(\mathbf{E}_{k+1}^f)^T \mathbf{E}_{k+1} \mathbf{U}_{k+1} \mathbf{E}_k^T \mathbf{E}_k^f = \mathbf{U}_{k+1}^{ff} \quad \text{and} \quad (\mathbf{E}_{k+1}^f)^T \mathbf{E}_{k+1} \mathbf{U}_{k+1} \mathbf{E}_k^T \mathbf{E}_k^u = \mathbf{U}_{k+1}^{fu} \quad (29)$$

using the orthogonality of the BLVs. Therefore, substitution into Eq. (22) yields

$$\hat{\epsilon}_{k+1}^f = \left( \mathbf{U}_{k+1}^{ff} - \mathbf{U}_{k+1}^{ff} \hat{\mathbf{K}}_k \mathbf{H}_k \mathbf{E}_k^f \right) \hat{\epsilon}_k^f \quad (30a)$$

$$5 \quad + \mathbf{U}_{k+1}^{ff} \hat{\mathbf{K}}_k \mathbf{v}_k - \hat{\mathbf{w}}_{k+1}^f \quad (30b)$$

$$+ \left( \mathbf{U}_{k+1}^{fu} - \mathbf{U}_{k+1}^{ff} \hat{\mathbf{K}}_k \mathbf{H}_k \mathbf{E}_k^u \right) \hat{\epsilon}_k^u. \quad (30c)$$

The terms (30a) and (30b) correspond to the standard recursion on the KF forecast error. When the filtered subspace is the entire state space,  $\mathbf{E}_k^f \triangleq \mathbf{E}_k$ , it is equivalent to a change of basis for the forecast error recursion in Eq. (14), written in the invariant dynamics for the BLVs.

10 The remaining term in the recursion on the filtered error is our primary object of interest. The term (30c) is fundamentally different from the relationship described by terms (30a) and (30b), which represents the usual stabilizing effect of the forecast-analysis cycle. Instead, Eq. (30c) describes two different processes: (i)  $\mathbf{U}_{k+1}^{ff} \hat{\mathbf{K}}_k \mathbf{H}_k \mathbf{E}_k^u$  is the correction in the filtered subspace, due to the sensitivity of these variables to observations in the unfiltered subspace, forward propagated to time  $t_{k+1}$ ; (ii)  $\mathbf{U}_{k+1}^{fu}$  represents the purely dynamical upwelling of the unfiltered error into the filtered variables. Generically  
 15  $\mathbf{U}_{k+1}^{fu} - \mathbf{U}_{k+1}^{ff} \hat{\mathbf{K}}_k \mathbf{H}_k \mathbf{E}_k^u \neq 0$  and  $\hat{\epsilon}_k^u$  is Gaussian distributed with covariance given by Eq. (26), thus is almost surely non-zero. This demonstrates that the *forecast error in the filtered subspace depends on the unfiltered error* via the forward evolution, whereas the *unfiltered error does not depend on the error in the filtered space*.

20 This implies that the direct application of EKF-AUS from perfect dynamics (Trevisan and Palatella, 2011b) to a noisy, linear system *systematically underestimates the uncertainty* in the span of the leading  $r$  BLVs. Specifically, EKF-AUS neglects the injection of the errors from the *trailing vectors*,  $\hat{\epsilon}_k^u$ , into the forecast of the leading vectors  $\hat{\epsilon}_{k+1}^f$ , represented in Eq. 30c. Even when uncertainty in the stable BLVs is bounded uniformly (Grudzien et al., 2017), error in the trailing BLVs *moves up* the Lyapunov filtration, and may cause filter divergence. In perfect, linear models, where uncertainty in the stable BLVs vanishes exponentially, the injection of error from the stable BLVs into the unstable subspace results in temporary mis-estimation though does not pose an issue to the asymptotic stability (Bocquet et al., 2017). However, with model error, the term (30c) demonstrates  
 25 that EKF-AUS must be augmented to correct a persistent underestimation.

It is important to note that the error in the unfiltered subspace moves upward through the backward Lyapunov filtration precisely because the unfiltered subspace is defined by the span of the trailing BLVs, governed by the invariant upper triangular dynamics. The span of the trailing BLVs is *not equal to* the direct sum of the trailing Oseledec spaces, which are themselves *covariant* with the dynamics. This choice for the unfiltered subspace comes naturally, however, as the filtered subspace (the  
 30 image space of  $\mathbf{K}_k$ ) is given by the span of the leading BLVs, equivalent to the span of the leading covariant Lyapunov vectors (Kuptsov and Parlitz, 2012, see Eq. 43).

The unfiltered subspace is uniquely defined (up to the inner product) as the *orthogonal complement* to the filtered space, i.e., the subspace in which the gain makes no correction in the analysis step. In ensemble data assimilation it has been demonstrated



numerically for perfect models, with weakly-nonlinear error growth, that the ensemble span of the ensemble Kalman filter and smoother typically aligns with the span of the unstable-neutral backward and covariant Lyapunov vectors (Ng et al., 2011; Bocquet and Carrassi, 2017), and thus the upwelling of unfiltered error may be considered a generic phenomena. In particular, we may consider a rank deficient EnKF to *sample the error statistics of an estimator which applies a rank deficient analysis update, confined to the span of the leading BLVs.*

In principle, data assimilation could be designed to prevent dynamical upwelling of unfiltered error by defining the unfiltered space to be the direct sum of the trailing, stable Oseledec spaces — in this case, unfiltered error would be covariant with the dynamics and leave the filtered error unaffected. Nevertheless, this design is artificial and would lead to poor filter performance: the orthogonal complement to the trailing Oseledec spaces, defining the filtered space, is equal to the span of the leading forward (or adjoint-covariant) Lyapunov vectors (Kuptsov and Parlitz, 2012, see Eq. 43), which has been shown not to contain the largest mass of the uncertainty (Ng et al., 2011). Furthermore, the dynamics in the forward Lyapunov vectors are defined by the QL factorization (Kuptsov and Parlitz, 2012), and the lower triangular propagator would transmit error from the filtered subspace to the unfiltered subspace, creating a *dynamic downwelling* which cannot be accounted for in the ensemble subspace. Defining the unfiltered space as the direct product of the stable, covariant Oseledec spaces would thus be contrary to the covariant dynamics and the properties of ensemble based covariances.

With the recursive form of the filtered error in Eq. (30), we directly compute the covariance of the filtered error, and the cross covariance of the filtered and unfiltered error, in the basis of BLVs. We define the operators

$$\Phi_{k+1} \triangleq \mathbf{U}_{k+1}^{\text{fu}} - \mathbf{U}_{k+1}^{\text{ff}} \hat{\mathbf{K}}_k \mathbf{H}_k \mathbf{E}_k^{\text{u}}, \quad (31)$$

$$\Sigma_k \triangleq \left[ \mathbf{I}_r - \hat{\mathbf{K}}_k \mathbf{H}_k \mathbf{E}_k^{\text{f}} \right] \hat{\mathbf{B}}_k^{\text{ff}} \left[ \mathbf{I}_r - \hat{\mathbf{K}}_k \mathbf{H}_k \mathbf{E}_k^{\text{f}} \right]^T + \hat{\mathbf{K}}_k \mathbf{R}_k \hat{\mathbf{K}}_k^T, \quad (32)$$

where  $\Phi_k$  is the operator which describes the propagation of unfiltered error into the filtered space and the operator  $\Sigma_k$  corresponds to the analysis error covariance for the standard KF, written in the basis of BLVs.

We first consider the recursion for the cross covariance. In particular, by combining Eq. (30) and Eq. (25), we obtain

$$\hat{\mathbf{B}}_{k+1}^{\text{fu}} = \Phi_{k+1} \hat{\mathbf{B}}_k^{\text{uu}} (\mathbf{U}_{k+1}^{\text{uu}})^T + \hat{\mathbf{Q}}_{k+1}^{\text{fu}} + \mathbf{U}_{k+1}^{\text{ff}} \left( \mathbf{I}_r - \hat{\mathbf{K}}_k \mathbf{H}_k \mathbf{E}_k^{\text{f}} \right) \hat{\mathbf{B}}_k^{\text{fu}} (\mathbf{U}_{k+1}^{\text{uu}})^T. \quad (33)$$

We now consider the covariance of the forecast error in the filtered variables. Using the identity in Eq. (32) we derive the recursion for the filtered error covariance  $\hat{\mathbf{B}}_{k+1}^{\text{ff}}$  as

$$\mathbf{B}_{k+1}^{\text{ff}} = \mathbf{U}_{k+1}^{\text{ff}} \Sigma_k (\mathbf{U}_{k+1}^{\text{ff}})^T + \hat{\mathbf{Q}}_{k+1}^{\text{ff}} \quad (34a)$$

$$+ \Phi_{k+1} \hat{\mathbf{B}}_k^{\text{uu}} \Phi_{k+1}^T \quad (34b)$$

$$+ \mathbf{U}_{k+1}^{\text{ff}} \left[ \mathbf{I}_r - \hat{\mathbf{K}}_k \mathbf{H}_k \mathbf{E}_k^{\text{f}} \right] \hat{\mathbf{B}}_k^{\text{fu}} \Phi_{k+1}^T \quad (34c)$$

$$+ \Phi_{k+1} \hat{\mathbf{B}}_k^{\text{uf}} \left[ \mathbf{I}_r - \hat{\mathbf{K}}_k \mathbf{H}_k \mathbf{E}_k^{\text{f}} \right]^T (\mathbf{U}_{k+1}^{\text{ff}})^T. \quad (34d)$$

When the filtered space is the whole space, i.e.,  $\mathbf{E}_k^{\text{f}} = \mathbf{E}_k$ , term (34a) entirely describes the evolution of the forecast error in the basis of BLVs — this is indeed just the forward propagation of the analysis error covariance for the KF. The term (34b)



represents the contribution of uncertainty from the unfiltered subspace, propagated via the  $\Phi_k$  operator, while terms (34c) and (34d) describe the forward evolution of the cross covariance of the uncertainty, into the filtered space.

### 3.3 Assimilation in the unstable subspace *exact* (AUSE)

Having derived the exact error covariance associated to the linear, sub-optimal estimator, which applies an analysis update  
 5 characteristic of the EnKF, we will summarize the result.

**Proposition 1.** *Assume that the initial forecast error,  $\epsilon_0$ , has mean zero and covariance  $\mathbf{B}_0$ . Let  $\mathbf{K}_k$  be defined as in Eq. (20) for all  $k$ , such that  $\mathbf{K}_k$  is the sub-optimal gain which makes corrections only in the span of  $\mathbf{E}_k^f$  (rank  $1 \leq r < n$ ). The forecast error, defined by Eq. (14), has covariance  $\mathbf{B}_k \triangleq \mathbf{E}_k \hat{\mathbf{B}}_k \mathbf{E}_k^T$ , defined recursively by*

$$\hat{\mathbf{B}}_k^{uu} = \hat{\mathbf{Q}}_k^{uu} + \mathbf{U}_k^{uu} \hat{\mathbf{B}}_{k-1}^{uu} (\mathbf{U}_k^{uu})^T, \quad (35a)$$

$$10 \quad \Phi_{k+1} = \mathbf{U}_{k+1}^{fu} - \mathbf{U}_{k+1}^{ff} \hat{\mathbf{K}}_k \mathbf{H}_k \mathbf{E}_k^u, \quad (35b)$$

$$\hat{\mathbf{B}}_{k+1}^{fu} = \Phi_{k+1} \hat{\mathbf{B}}_k^{uu} (\mathbf{U}_{k+1}^{uu})^T + \hat{\mathbf{Q}}_{k+1}^{fu} + \mathbf{U}_{k+1}^{ff} \left( \mathbf{I}_r - \hat{\mathbf{K}}_k \mathbf{H}_k \mathbf{E}_k^f \right) \hat{\mathbf{B}}_k^{fu} (\mathbf{U}_{k+1}^{uu})^T, \quad (35c)$$

$$\Sigma_k = \left[ \mathbf{I}_r - \hat{\mathbf{K}}_k \mathbf{H}_k \mathbf{E}_k^f \right] \hat{\mathbf{B}}_k^{ff} \left[ \mathbf{I}_r - \hat{\mathbf{K}}_k \mathbf{H}_k \mathbf{E}_k^f \right]^T + \hat{\mathbf{K}}_k \mathbf{R}_k \hat{\mathbf{K}}_k^T, \quad (35d)$$

$$\begin{aligned} \hat{\mathbf{B}}_{k+1}^{ff} = & \mathbf{U}_{k+1}^{ff} \Sigma_k (\mathbf{U}_{k+1}^{ff})^T + \hat{\mathbf{Q}}_{k+1}^{ff} + \Phi_{k+1} \hat{\mathbf{B}}_k^{uu} \Phi_{k+1}^T \\ & + \mathbf{U}_{k+1}^{ff} \left[ \mathbf{I}_r - \hat{\mathbf{K}}_k \mathbf{H}_k \mathbf{E}_k^f \right] \hat{\mathbf{B}}_k^{fu} \Phi_k^T + \Phi_k \hat{\mathbf{B}}_k^{uf} \left[ \mathbf{I}_r - \hat{\mathbf{K}}_k \mathbf{H}_k \mathbf{E}_k^f \right]^T (\mathbf{U}_{k+1}^{ff})^T. \end{aligned} \quad (35e)$$

15

**Definition 3.** *Equation (35) is defined to be the Kalman Filter, Assimilation in the Unstable Subspace Exact (KF-AUSE) Riccati equation, for a filtered subspace of dimension  $r$ .*

It should be noted that the KF-AUSE Riccati equation is also valid for the true forecast error covariance in perfect models, where  $\mathbf{Q}_k \triangleq \mathbf{0}_n$  for all  $k$ . Let  $r = n_0$ ,  $\mathbf{Q}_k \triangleq \mathbf{0}_n$  and  $\mathbf{P}_k \triangleq \mathbf{E}_k^f \Gamma_k (\mathbf{E}_k^f)^T$  be defined as the *estimated* forecast error covariance  
 20 for EKF-AUS, then the recursion is defined by

$$\Gamma_{k+1} \triangleq \mathbf{U}_{k+1}^{ff} \left[ \mathbf{I}_r - \hat{\mathbf{K}}_k \mathbf{H}_k \mathbf{E}_k^f \right] \Gamma_k \left[ \mathbf{I}_r - \hat{\mathbf{K}}_k \mathbf{H}_k \mathbf{E}_k^f \right]^T (\mathbf{U}_{k+1}^{ff})^T + \mathbf{U}_{k+1}^{ff} \hat{\mathbf{K}}_k \mathbf{R}_k \hat{\mathbf{K}}_k^T (\mathbf{U}_{k+1}^{ff})^T, \quad (36)$$

analogous to term (34a). Comparing Eq. (35) and Eq. (36), we see that even in perfect models the estimated error covariance of EKF-AUS in the filtered subspace and the true error covariance do not agree, i.e.,  $\Gamma_{k+1} \neq \hat{\mathbf{B}}_{k+1}^{ff}$ . This is because the estimated AUS error in Eq. (36) neglects the upwelling of the *initial error* in the unfiltered subspace, described by terms (34b), (34c)  
 25 and (34d). However, in this case, the unfiltered initial error decays exponentially and the mis-estimation in the filtered space doesn't threaten filter stability: the AUS estimated error covariance converges to the true error in its asymptotic limit (Bocquet et al., 2017).



### 3.4 Discussion

In ideal, linear models, the KF-AUSE Riccati equation (35) describes the *exact* evolution of the forecast error decomposed into a basis of BLVs, where a sub-optimal gain applies the Bayesian update with respect to an arbitrary number,  $r$ , of the leading basis vectors. Although the analysis update in Eq. (20) is sub-optimal, and defined via a rank deficient filtered subspace, the 5 recursion in Eq. (35) has no mis-estimation of its error statistics. We emphasize, however, that the KF-AUSE Riccati equation (35) is *not intended to provide a computational advantage* — its computation requires knowledge of error in the unfiltered subspace and, in nonlinear models, a *full rank representation* of the tangent linear dynamics. Nonetheless, this recursion is demonstrative of an important concept: in a reduced rank estimator that applies its analysis update in the span of the leading BLVs, the true error in the same span *will always depend on the unfiltered error* in the trailing vectors.

10 The upwelling of uncertainty from the unfiltered subspace to the filtered ensemble span thus explains one of the dynamical mechanisms determining the intrinsic role of covariance inflation in a reduced rank EnKF, providing a theoretical motivation for its use to prevent filter divergence. If one wishes to correct the error in the span of the leading BLVs exactly, it requires calculating the covariance of the unfiltered error as well as the cross covariance of the error in the filtered and unfiltered subspaces as in Eq. (35). In practical applications, one must find a suitable approximation of the upwelling phenomenon to 15 prevent the systematic underestimation of the forecast error, and/or, extend the rank of the correction to control the transient growth of errors in the stable modes.

Reduced rank Kalman filters have previously corrected for the upwelling of model errors with covariance inflation methods. For instance, although it was not explicitly formulated as such, the SEEK filter of Pham et al. (1998) can be seen to compensate for model errors originating in the unfiltered, stable subspace: while components of the model error covariance which 20 are orthogonal to the filtered subspace are left neglected, there is implicit treatment by utilizing its forgetting factor to inflate the variance of the estimated error in the filtered subspace (Nerger et al., 2005). The contribution of the unfiltered error to the estimated error was also studied in ensemble methods by Raanes et al. (2015), in which the authors explored sampling methodology to compensate for the unresolved model errors, residing outside of the ensemble span. Our work adds to this discussion, now highlighting the *explicit mechanism* which necessitates these covariance inflation techniques under a rank deficient gain.

25 The dynamical upwelling of model error differs from the sampling errors induced by nonlinear dynamics in perfect models, treated in the modified EKF-AUS-NL (Palatella and Trevisan, 2015) and in the finite size ensemble Kalman filter, (**EnKF-N**) (Bocquet, 2011; Bocquet et al., 2015). Rather, we have shown that the upwelling of the unfiltered error through the Lyapunov filtration acts as a linear effect and is acute in the presence of additive model errors which are excited by transient instabilities. While the effect of the dynamical upwelling could be neglected in perfect models (Bocquet et al., 2017), the work of Grudzien 30 et al. (2017) has demonstrated that transient instability in the span of the stable BLVs can drive the unfiltered error to become impractically large — furthermore, this error is transmitted into the filtered subspace, driving filter divergence if it is left uncorrected. However, the significance of results with AUS in perfect models is not lost: if the dimension of the filtered space is sufficiently large, such that dynamical stability in the unfiltered subspace is strong enough to rapidly dissipate errors, the effect of the upwelling may become negligible.



Uncorrected forecast errors leading to filter divergence has been previously studied in the context of perfect, nonlinear models, with an important connection to our above discussion: if an EnKF applies a correction of rank less than the number of unstable and neutral Lyapunov exponents, it has been found the filter's estimated error can become small while the filter permanently loses track of the true trajectory (Ng et al., 2011). This behavior is easily understood in terms of the filter's 5 failure to correct the error growth in the span of at least one of the unstable-neutral BLVs. For large geophysical models, where ensemble based covariances may be extremely rank deficient, hybridized gains have been shown to account for the failure of ensemble based gain to correct the error in the span of all the unstable-neutral BLVs (Penny, 2017). In hybridization the ensemble-based estimated error covariance is augmented by a static, climatological estimate — using the climatological covariance, the rank of the estimator used for the analysis update is increased, and has the effect of applying a correction 10 to additional modes outside of the ensemble span (Hamill and Snyder, 2000). The need to rectify the rank deficiency of the ensemble based Kalman gain takes on a new significance given our understanding of the dynamical upwelling of uncertainty. In the presence of model error, even when the ensemble rank is greater than the number of unstable-neutral Lyapunov exponents, a hybridized gain or additive inflation (Whitaker and Hamill, 2012) may improve filter performance by keeping the errors in the span of the weakly stable BLVs small, diminishing the effect of their transient growth and upwelling.

15 Multiplicative inflation, acting only within the ensemble span, can rectify the under-estimation of uncertainty in the filtered subspace, due to neglecting the effect of the upwelling of error. For example, the linear form of EKF-AUS does not include the upwelling of unfiltered error in its estimated covariance — inclusion of multiplicative inflation to the estimated error covariance compensates for the upwelling of unfiltered errors which is not represented in the recursion for EKF-AUS, and simulates the terms (34b), (34c) and (34d) in the KF-AUSE recursion. Multiplicative inflation may also be used to account 20 for mis-estimation of forecast errors resultant from nonlinear evolution, but this mis-estimation may also be accounted for using less ad hoc approaches including parameterizing this error with hyperpriors (Bocquet et al., 2015). We argue that the hyperprior in EnKF-N can, in principle, also be selected to take into account the structure of the ideal posterior for the reduced rank estimator, in the presence of model error, described by KF-AUSE (see also the discussion at the end of section 4.2).

25 Whitaker and Hamill (2012) hypothesized that additive inflation could better compensate for the effects of unresolved model error, while multiplicative inflation is best suited to account for sampling error, consistent with what was noted by Bocquet (2011) and Bocquet and Sakov (2012). This hypothesis is supported by our results and the above discussion: the combination of rank deficiency of the analysis and the presence of additive model error determines an intrinsic role for covariance inflation in ensemble based Kalman filters in chaotic, dynamical systems, due to the upwelling of unfiltered errors. However, our above 30 discussion also highlights how the need for inflation can be mitigated by: (i) sufficiently increasing the ensemble size (Grudzien et al., 2017); (ii) rectifying the rank deficiency of the analysis update via hybridization (Penny, 2017); (iii) utilizing a hyperprior which takes into account the dynamical upwelling and mis-estimation of error (Bocquet et al., 2015); or (iv) some combination of the above. In the following section, we numerically explore the effects of stability, transient instability, and the strength therein, on filter divergence and the need for covariance inflation with reduced rank estimators.



## 4 Numerical results

### 4.1 Experimental setup

Numerically studying the KF, we construct a discrete, linear model from the **Lorenz 96 equations (L96)** (Lorenz and Emanuel, 1998). For each  $m \in \{1, \dots, n\}$  the (L96) equations read  $\frac{dx}{dt} \triangleq \mathbf{L}(\mathbf{x})$ ,

5  $L_m(\mathbf{x}) = -x_{m-2}x_{m-1} + x_{m-1}x_{m+1} - x_m + F \quad (37)$

such that the components of the vector  $\mathbf{x}$  are given by the variables  $x_m$  with periodic boundary conditions,  $x_0 = x_n$ ,  $x_{-1} = x_{n-1}$  and  $x_{n+1} = x_1$ . The term  $F$  in L96 is the forcing parameter. The tangent linear model (Kalnay, 2003) is governed by the equations of the Jacobian,  $\nabla_{\mathbf{x}}\mathbf{L}(\mathbf{x})$ ,

$$\nabla_{\mathbf{x}}L_m(\mathbf{x}) = (0, \dots, -x_{m-1}, x_{m+1} - x_{m-2}, -1, x_{m-1}, 0, \dots, 0). \quad (38)$$

10 In *linear experiments*, we fix the system dimension  $n \triangleq 10$ , and the linear propagator in our model  $\mathbf{M}_k$  is generated by computing the discrete, tangent linear model from the resolvent of the Jacobian equation, Eq. (38): This linear model satisfies Oseledec's theorem by construction (Barreira and Pesin, 2002). In generating the discrete, tangent linear model, the discretization time between observations is fixed at  $\delta_k \triangleq 0.1$  for all  $k$ . We numerically integrate the Jacobian equation with a fourth order Runge-Kutta scheme with a time step of  $h \triangleq 0.01$ . The observational error covariance  $\mathbf{R}_k$ , model error covariance  $\mathbf{Q}_k$   
 15 and observation operator  $\mathbf{H}_k$  are all fixed as the identity  $\mathbf{I}_{10}$ , for simplicity, in this setup.

In our *nonlinear experiments* with the extended Kalman filter (**EKF**) (Jazwinski, 1970), we use Eq. (37) directly for our model state evolution, and fix the state dimension to  $n \triangleq 40$ . The nonlinear trajectory is integrated with a step size of  $h \triangleq 0.05$ , with an interval between observation times of  $\delta_k \triangleq 0.1$ . At each observation time, before observations are given, the true trajectory is perturbed by additive Gaussian noise with a proscribed covariance  $\mathbf{Q}$ , fixed in time. The matrix  $\mathbf{Q}$  defined by the  
 20 circulant matrix with  $c_0 = 0.5, c_1 = 0.25, c_2 = 0.125, c_{39} = 0.25, c_{38} = 0.125$  and all other entries zero,

$$\mathbf{Q} \triangleq \begin{pmatrix} c_0 & c_{39} & \cdots & c_2 & c_1 \\ c_1 & c_0 & c_{39} & & c_2 \\ \vdots & c_1 & c_0 & \ddots & \vdots \\ c_{38} & & \ddots & \ddots & c_{39} \\ c_{39} & c_{38} & \cdots & c_1 & c_0 \end{pmatrix}. \quad (39)$$

The choice of the circulant matrix reflects the stationary statistics and periodic nature of the L96 model, and the fact that we wish to highlight the effect of analytically resolving complex model error. The observational error covariance matrix is fixed as  $0.25 * \mathbf{I}_{40}$ , the scalar matrix with eigenvalue 0.25. The observation operator is fixed in time as  $\mathbf{H}_k \triangleq \mathbf{I}_{40}$ .

25 

### 4.2 Linear Kalman filter

In a linear setting, we compute the forecast error covariance of KF-AUSE via the recursive Riccati equation, Eq. (35), and compare it with that of the KF, for which the filtered space is the entire model space. This illustrates the ideal performance

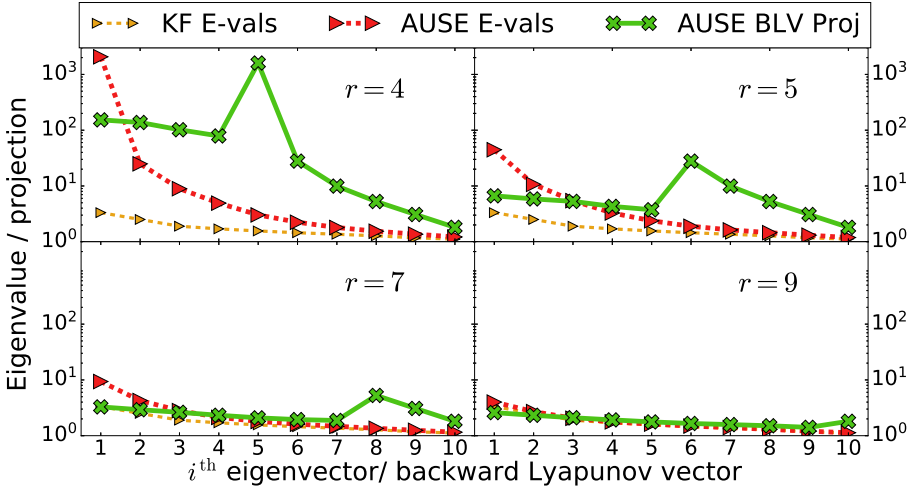


**Figure 1.** Eigenvalues of the KF and KF-AUSE forecast error covariance plotted with triangles. Projection coefficients of the KF-AUSE forecast error covariance plotted with X's. Dimension of the KF-AUSE filtered subspace is  $r$ . Note the log scale of the  $y$ -axis.

of a rank deficient, sub-optimal filter *without estimation errors*; we compare this relative to a full rank correction, where the sub-optimal filter applies corrections only to the leading  $r$  BLVs and the forecast error is treated analytically. We compute the average eigenvalues of the forecast covariance matrix for each the KF and KF-AUSE over 100,000 parallel forecast cycles and examine the stratification of the uncertainty in a basis of BLVs, i.e., how strongly the covariance projects into each direction.

5 Specifically, for both the KF and KF-AUSE we compute the average projection coefficient of the forecast error covariance into the  $i$  th BLV at each forecast time,  $(\mathbf{E}_k^i)^T \mathbf{B}_k \mathbf{E}_k^i$ , and average this coefficient over  $k$ .

In order to visualize the full spectrum of the forecast error covariance, we use the 10 dimensional discrete, tangent-linear model of L96 as the linear model for our KF-AUSE experiments. For the standard forcing value of  $F = 8$ , there are three unstable, one neutral, and six stable Lyapunov exponents, i.e.,  $n_0 = 4$ . In Fig. 1, the averaged eigenvalues of the KF and KF-10 AUSE forecast error covariance are plotted, with triangle markers, differentiated by color. In each subplot, the KF remains the same but we vary the dimension of the filtered subspace,  $r$ , for KF-AUSE.

In the top left panel of Fig. 1 the number of corrected modes is equal to  $n_0$ , corresponding to correcting the error in the unstable-neutral subspace. Here, the leading eigenvalue of the forecast uncertainty of KF-AUSE is orders of magnitude above the forecast uncertainty in the KF. This should be contrasted with perfect models where, asymptotically, there can only be four 15 non-zero eigenvalues, and under generic conditions, the KF and EKF-AUS will coincide (Bocquet et al., 2017). In accordance with the results of Grudzien et al. (2017), correcting the first stable mode ( $r = 5$ ) brings a substantial reduction in forecast uncertainty (see top right Fig. 1). We see the forecast uncertainty likewise diminishes as each additional mode is corrected, as the KF-AUSE covariance converges to that of the KF.

It is of special interest how the projection coefficients of the forecast error covariance relates to the dimension of the filtered 20 subspace,  $r$ . In the KF, the projection coefficients are closely aligned with the eigenvalue profile, descending in the order of



the Lyapunov exponents, and this line is not pictured due to the redundancy. However, in the forecast error covariance of KF-AUSE, the leading *uncorrected stable mode* is the dominant direction for the uncertainty among the BLVs, systematically across  $n_0 \leq r < n$ , with projection coefficient on the order of the leading eigenvalue. This distinguishes the setting of additive model error from perfect models where the projection coefficients of the forecast error covariance in the stable BLVs will be 5 zero asymptotically (Gurumoorthy et al., 2017). In a straightforward implementation of KF-AUS in the presence of model error, which neglects corrections to the weakly stable modes and the upwelling of the unfiltered error on the order of the uncertainty in  $\mathbf{B}_k^{n_0+1}$ , this unfiltered error will furthermore transmit into the filtered subspace, driving filter divergence.

The structure of the forecast error covariance of KF-AUSE, revealed in the basis of BLVs, has special significance for the rank deficient EnKF. Particularly, we may understand the covariance of KF-AUSE to express the ideal forecast error of the rank 10 deficient EnKF, and should guide any independent, identically distributed (**iid**) sampling scheme which represents this error distribution. The hyperprior in EnKF-N (Bocquet et al., 2015), used to describe the mis-estimation of the true error statistics from a finite iid draw of samples, may also incorporate the structure of the ideal posterior under a rank deficient gain. Similarly to how the hyperprior for the covariance in EnKF-N is restricted to the cone of positive semi-definite symmetric matrices in perfect models, its extension to additive model error may incorporate a restriction to the covariance matrices which share the 15 stratification of uncertainty expressed in KF-AUSE. Likewise, when unfiltered error is known to be large, the structure of the KF-AUSE covariance demonstrates the benefit of hybridization to rectify the rank deficiency: even if the hybrid gain induces sampling error by corrupting the recursion for the estimated error, controlling the unfiltered error by some means can diminish the leading order source of uncertainty.

#### 4.3 Extended Kalman filter with nonlinear model dynamics

20 In our nonlinear experiments, we compute the analysis root mean square error (**RMSE**) of each the (i) full rank extended Kalman filter (**EKF**), (ii) EKF-AUS and (iii) EKF-AUSE, for which Eq. (35) is used to compute the estimated covariance and rank  $r$  gain. We will study the effect of analytically resolving the unfiltered error as compared with the straightforward implementation of EKF-AUS, which will make no correction to account for the unfiltered error complementary to the anomaly subspace.

25 Recall that EKF-AUS so far has only been studied in the perfect model scenario — we implement EKF-AUS in the presence of model error by computing a rank  $r$  estimated error covariance, which includes the projection of the model error covariance,  $\mathbf{Q}_k$  into the span of the leading BLVs in the forecast Riccati equation, i.e.  $(\mathbf{E}_k^f)^T \mathbf{Q}_k \mathbf{E}_k^f = \hat{\mathbf{Q}}_k^{ff}$ . This corresponds to utilizing only the first line of the recursion for  $\hat{\mathbf{B}}_k^{ff}$ , Eq. (34a), to compute the estimated forecast error covariance of EKF-AUS. The implementation of EKF-AUSE thus differs by utilizing a *full rank* ensemble of anomalies to compute the complete Riccati 30 equation, Eq. (35). We utilize this  $n$  dimensional covariance equation to compare the effect of the additional inflation, by including the terms in Eq. (34b), Eq. (34c) and Eq. (34d) in the correction to the filtered space, on the performance of filter RMSE.

We study the performance of EKF-AUS/E when the dimension of the filtered subspace is *greater than*, or equal to, the dimension of the unstable-neutral subspace; the case  $r < n_0$  will trivially lead to divergence (Bocquet et al., 2017). For the 40



dimensional L96, with standard forcing  $F = 8$ ,  $n_0 = 14$ , with one neutral Lyapunov exponent. In Fig. 2, we plot the analysis RMSE of EKF-AUS and EKF-AUSE with triangles and X's respectively, while we vary over the dimension of the filtered subspace, with the RMSE computed over 100,000 analysis cycles.

To benchmark the performance of EKF-AUS/E, we plot the observational error standard deviation and the analysis RMSE of the standard, full rank EKF in horizontal lines — the algorithms for EKF-AUS/E are tantamount to a change of basis for the EKF when the filtered subspace is equal to the full space, and thus this is the logical point of comparison. We are interested in finding the necessary dimension of the filtered subspace such that EKF-AUS/E has an RMSE which: (i) performs better than the observational error standard deviation and (ii) performs comparably to filtering the entire space. When the RMSE of EKF-AUS/E falls below the observational error standard deviation, the filter has a forecast performance superior to initializing observations directly in the model; when it performs closely to the EKF, the filter can be considered close to optimal performance, while utilizing a sub-optimal correction based on only  $r < n$  directions.

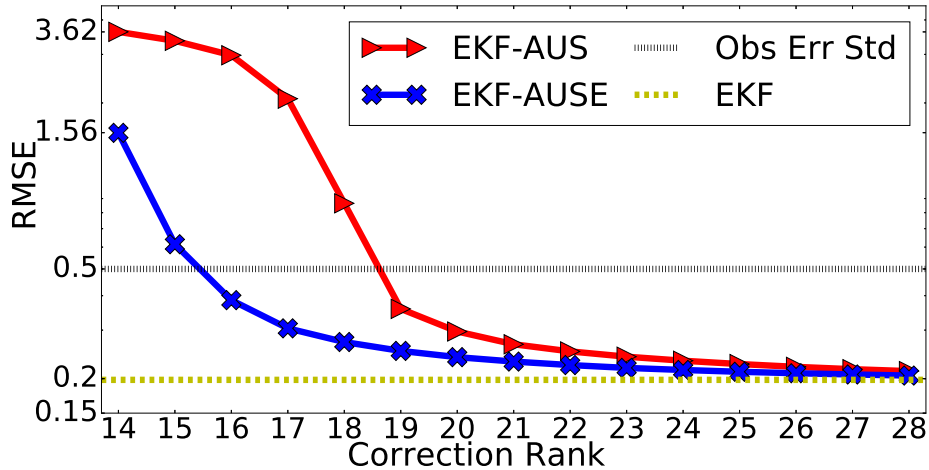


**Figure 2.** Analysis RMSE of EKF-AUS plotted with triangles and EKF-AUSE plotted with X's, varying over the rank of the sub-optimal gain. Horizontal lines are the observational error standard deviation and EKF analysis RMSE. Note the log scale of the y-axis.

In Fig. 2, when the dimension of the filtered subspace for both AUS/E reaches 28 the difference between both EKF-AUS/E and the full-rank EKF becomes negligible. The fact that EKF-AUS obtains near optimal performance, representing the uncertainty in the leading  $r = 28$  BLVs while neglecting the remaining, corroborates the claim of Grudzien et al. (2017): in the presence of model noise, the filter correction should also incorporate weakly stable directions that can be instantaneously unstable. It is of particular interest, however, that the convergence of EKF-AUSE to the skill of the full rank EKF is substantially faster: EKF-AUSE obtains adequate filter performance (RMSE lower than observational error standard deviation) by correcting only 16 BLVs while EKF-AUS requires a correction of rank 19. For other scalings of the matrix  $\mathbf{Q}$ , multiplying  $\mathbf{Q}$  by .1, .2, 1.5, 2, and by varying the time between observations, e.g.  $\delta_k = .01$  or .5 we obtain similar results, not pictured here. The profiles of the curves in Fig. 2 are similar across these experimental configurations: the RMSE of EKF-AUSE is improved



over EKF-AUS by including the analytical inflation factor, and the RMSE approaches an adequate/optimal level with a smaller dimension for the filtered space. This pattern demonstrates that including the inflation factor to the filtered subspace, resolving the upwelling of the unfiltered error, reduces the necessary ensemble rank to obtain a stable filter. We emphasize again that EKF-AUSE does not represent a computational advantage as a *full rank* set of perturbations is used to describe the analytic 5 form for the upwelling of the error.

To explain the convergence of EKF-AUS, which doesn't account for the unfiltered subspace, to the full rank EKF, we look at the behavior of the local Lyapunov exponents for the L96 model. In Fig. 3 we show the box plot statistics of the local Lyapunov exponents for exponents 14 through 28 of the L96 model. Exponent  $\lambda_{14} = 0$ , and the remaining pictured exponents correspond to the leading, stable BLVs. We emphasize that the local Lyapunov exponents of  $\lambda_{15}$  through  $\lambda_{18}$ , though having negative 10 mean, are sufficiently unstable locally such that EKF-AUS diverges when it disregards the upwelling of the error from these asymptotically stable modes.

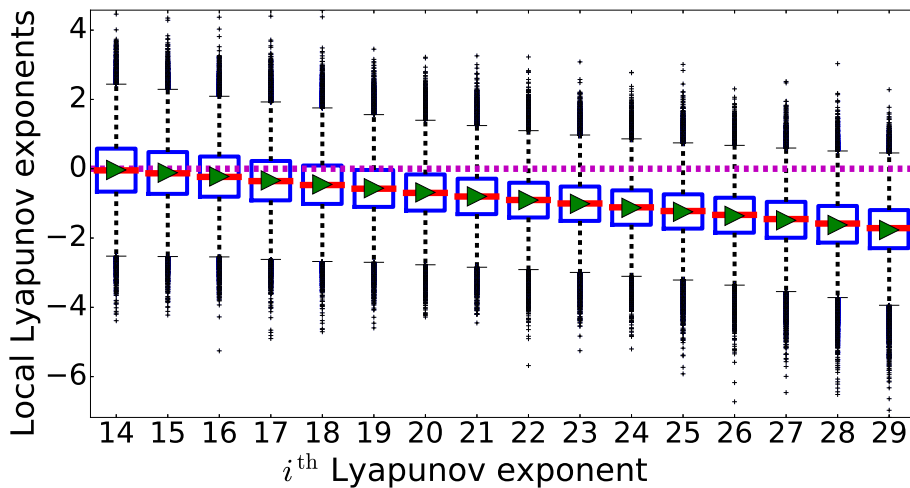


**Figure 3.** Box plot statistics of the local Lyapunov exponents, for Lyapunov exponents 14 through 24, over 100,000 realizations for the 40 dimensional L96 model. The mean ( $i$  th Lyapunov exponent) is plotted as a triangle with median the horizontal line. Box contains inner two quartiles of realizations, with whiskers extending to 1.5 the inner quartile width from the third and first quartile. Outliers are realizations outside of this range, plotted individually.

When the filtered subspace for EKF-AUS is of dimension 19, such that the leading *unfiltered* BLV corresponds to  $\lambda_{20}$ , all unfiltered Lyapunov exponents have over 75% of local realizations strictly stable; this corresponds to the rank when EKF-AUS has adequate performance. Likewise, the difference between EKF-AUS/E and the EKF is negligible when the leading unfiltered 15 BLV corresponds to  $\lambda_{29}$ , with only 1.51% of its local realizations being non-negative. These findings are consistent with the results in Grudzien et al. (2017): in the presence of model error, unconstrained forecast error is strongly forced by the error in BLVs, which are asymptotically stable but, that experience strong and frequent local instability.



Finally, we are interested in how analytically computing the upwelling of error from the unfiltered subspace, as in EKF-AUSE, compares with a homogeneous, multiplicative inflation applied to the EKF-AUS algorithm. Multiplicative scalar inflation is among the most common approaches to mitigate for sampling and model error in Kalman filtering methods, and it is widely used in operational environmental forecasts utilizing the EnKF (Whitaker and Hamill, 2012). In our experiments, if  $\mathbf{P}_k \triangleq (\mathbf{E}_k^{\text{ff}})^T (\Psi_k + \hat{\mathbf{Q}}_k^{\text{ff}}) \mathbf{E}_k^{\text{ff}}$  is the estimated forecast error of EKF-AUS, we define the inflated covariance  $\mathbf{P}_k^I$  as  $\mathbf{P}_k^I = (\mathbf{E}_k^{\text{ff}})^T (\alpha \Psi_k + \hat{\mathbf{Q}}_k^{\text{ff}}) \mathbf{E}_k^{\text{ff}}$  for some chosen scalar  $\alpha$ . The inflated covariance  $\mathbf{P}_k^I$  is used to compute the sub-optimal gain, as a simple way to compensate for the underestimation of the forecast error when using the recursion in Eq. (34a).

From the results in Fig. 2, we select the dimension of the filtered subspace to be 17, such that EKF-AUSE has RMSE below the observational error standard deviation while EKF-AUS (without inflation) has diverged. In Fig. 4, we plot the analysis RMSE of EKF-AUSE, with filtered subspace dimension 17, the observational error standard deviation and the full-rank EKF analysis RMSE as in Fig. 2 as horizontal lines. Additionally, we plot the analysis RMSE of EKF-AUS as a function of the inflation value applied to the forecast error covariance, with the inflation values plotted as triangles. The RMSE of all the above is again computed over 100,000 forecast cycles.

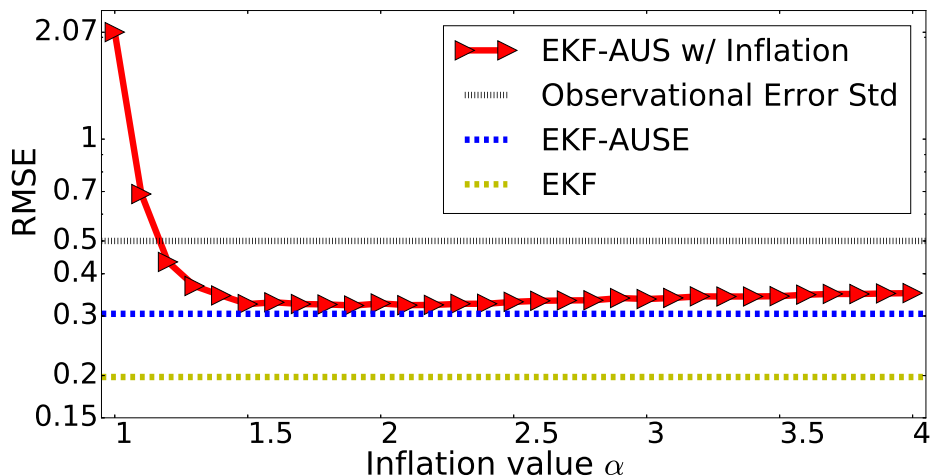


**Figure 4.** Analysis RMSE of EKF-AUS, correction rank 17, with multiplicative inflation plotted versus the inflation value. Horizontal lines are the observational error standard deviation, EKF-AUSE and EKF analysis RMSE. Note the log scale of the *y*-axis.

Figure 4 highlights distinctly the impact of including multiplicative inflation to EKF-AUS: the performance of EKF-AUS with inflation quickly becomes comparable to the analytically resolved EKF-AUSE, which in this case, represents the lower-most bound for the RMSE of EKF-AUS with homogeneous inflation. Figure 4 confirms the role of multiplicative inflation as compensating for the upwelling of unfiltered error under weakly-nonlinear error growth, and explains the underlying dynamical mechanism: multiplicative inflation brings the estimated forecast error covariance of EKF-AUS closer to the ideal covariance given by EKF-AUSE.



It is important to remark that the analytic form for the inflation in Eq. (35) is only a useful representation for the weakly nonlinear evolution of error; for more nonlinear error evolution, multiplicative inflation will also compensate for the sampling error as described by Palatella and Trevisan (2015), and the performance of EKF-AUSE is not expected to provide a bound in this regime. The ways that multiplicative inflation can mitigate the nonlinear sources of error are discussed by, e.g., Bocquet 5 (2011); Bocquet et al. (2015). Table 1 summarizes the reasons for multiplicative inflation within different dynamical regimes. Figure 5 gives a conceptual diagram of the number of samples needed to prevent divergence of the EnKF in different dynamical regimes, and the effect of multiplicative inflation on this requirement.

## 5 Conclusions

Assimilation in the Unstable Subspace (**AUS**) has provided a useful conceptual framework for understanding the dynamical 10 properties of data assimilation cycling in perfect models. Both numerical and mathematical results have confirmed the underlying hypothesis of Anna Trevisan: in the setting of perfect, chaotic models, the evolution of uncertainty is confined to a space characterized by non-negative Lyapunov exponents, typically of much lower dimension than the full model state space (Palatella et al., 2013). In ensemble data assimilation, we see that the asymptotic characteristics of the anomalies exhibit these 15 properties, which can be exploited to reduce the computational burden of the assimilation cycle (Bocquet and Carrassi, 2017). This phenomena has recently also been exploited to reduce the numerical cost of synchronization in dynamical shadowing based data assimilation methods (de Leeuw et al., 2017).

This paper demonstrates that the framework of AUS can likewise be used to understand the underlying mechanisms for the evolution of uncertainty in reduced rank filters applied to chaotic dynamics in the presence of additive model error. Due to the high dimensional models, and unresolved physical processes, this circumstance is ubiquitous in high-dimensional geoscience 20 applications where standard EnKFs are extremely rank deficient. Utilizing the Lyapunov filtration for the backward vectors, we have shown how unfiltered error, outside of the span of the anomalies, is transmitted by the dynamics into the filtered subspace. In perfect models, or when stability in the unfiltered subspace is sufficiently strong, this effect can be neglected due to the rapid dissipation of unfiltered errors. However, Grudzien et al. (2017) demonstrate how weakly stable modes of high variance can 25 go through periods of transient instability, exciting unfiltered error. The dynamic upwelling of unfiltered error, characterized by the term (30c), acts as a linear effect on filters with small ensemble sizes. Under weakly-nonlinear error growth, the span of the anomalies projects strongly onto the span of the leading BLVs — therefore, the Riccati equation, Eq. (35), highlights an important, and previously unexplained, mechanism driving the need for covariance inflation in reduced rank, ensemble based Kalman filters.

The role of inflation we describe differs from previous studies, e.g., the work of Palatella and Trevisan (2015), which 30 studied the nonlinear interactions of error in perfect models. The phenomena of dynamical upwelling is also independent of the mis-estimation of error due to a finite sample size representing the true error statistics (Bocquet et al., 2015). Rather, we exhibit an effect which can contribute to filter divergence over short time scales in ensemble data assimilation, when the error dynamics are linear or weakly-nonlinear, if uncertainty is forced by additive model errors. This persistent dynamical upwelling



of errors from the unfiltered space into the ensemble subspace is a phenomena which we prove analytically in linear models, and demonstrate numerically to be a valid approximation of weakly-nonlinear error growth in nonlinear models for reduced rank extended Kalman filters. The KF-AUSE Riccati equation, Eq. (35), therefore represents the ideal recursion for the error covariance of a reduced rank Kalman filter.

5 If we treat the standard EnKF as Monte Carlo estimate of the error statistics characteristic of the KF-AUSE covariance, the ideal uncertainty for a reduced rank Kalman filter, the dynamical upwelling explains the intrinsic role for covariance inflation in the reduced rank EnKF. But in addition, our work also confirms that the role of covariance inflation may potentially be mitigated by: (i) sufficiently increasing the ensemble size to include asymptotically stable modes that produce transient instabilities, such that unfiltered error is rapidly dissipated by stable dynamics; (ii) increasing the rank of the analysis update 10 itself, with a hybridized gain; (iii) parameterizing the upwelling of error via a hyperprior which targets the ideal evolution true forecast error; or (iv) some combination of the above. Our new understanding of the dynamics of error propagation thus opens new opportunities in algorithm design, where the above techniques may be used directly to ameliorate the effects of dynamical upwelling.

Where there is dynamical chaos, AUS will continue to be a robust framework for the theory of data assimilation in physical 15 models. Understanding the dynamical mechanisms that govern the evolution of error in fully nonlinear data assimilation, e.g., the unstable-neutral manifolds of the (stochastic) chaotic attractor, will be the subject of future research and may be considered the logical extension of the framework put forward by Anna Trevisan — her insight to the underlying processes in assimilation will continue to provide inspiration to both developers and practitioners of data assimilation methods.

*Acknowledgements.* This work benefited from funding by the project REDDA of the Norwegian Research Council under contract 250711. 20 Cerea is a member of the Institut Pierre-Simon Laplace (IPSL). The authors would like to show their gratitude and respect for Anna Trevisan, and the impact she has had on the understanding of theoretical data assimilation.



## References

Barreira, L. and Pesin, Y.: Lyapunov Exponents and Smooth Ergodic Theory, Student Mathematical Library, American Mathematical Society, 2002.

Benettin, G., Galgani, L., Giorgilli, A., and Strelcyn, J.: Lyapunov characteristic exponents for smooth dynamical systems and for Hamiltonian systems; a method for computing all of them. Part 1: Theory, *Meccanica*, 15, 9–20, 1980.

Bocquet, M.: Ensemble Kalman filtering without the intrinsic need for inflation, *Nonlinear Processes in Geophysics*, 18, 735–750, 2011.

Bocquet, M. and Carrass, A.: Four-dimensional ensemble variational data assimilation and the unstable subspace, *Tellus A*, 69, 1304 504, 2017.

Bocquet, M. and Sakov, P.: Combining inflation-free and iterative ensemble Kalman filters for strongly nonlinear systems, *Nonlinear Processes in Geophysics*, 19, 383–399, 2012.

Bocquet, M., Raanes, P., and Hannart, A.: Expanding the validity of the ensemble Kalman filter without the intrinsic need for inflation, *Nonlinear Processes in Geophysics*, 22, 645, 2015.

Bocquet, M., Gurumoorthy, K., Apte, A., Carrass, A., Grudzien, C., and Jones, C.: Degenerate Kalman Filter Error Covariances and Their Convergence onto the Unstable Subspace, *SIAM/ASA Journal on Uncertainty Quantification*, 5, 304–333, 2017.

Carrass, A., Trevisan, A., and Ubaldi, F.: Adaptive observations and assimilation in the unstable subspace by breeding on the data-assimilation system, *Tellus A*, 59, 101–113, 2007.

Carrass, A., Trevisan, A., Descamps, L., Talagrand, O., and Ubaldi, F.: Controlling instabilities along a 3DVar analysis cycle by assimilating in the unstable subspace: a comparison with the EnKF, *Nonlinear Processes in Geophysics*, 15, 503–521, 2008.

Carrass, A., Vannitsem, S., Zupanski, D., and Zupanski, M.: The maximum likelihood ensemble filter performances in chaotic systems, *Tellus A*, 61, 587–600, 2009.

Chandrasekar, J., Kim, I., Bernstein, D., and Ridley, A.: Cholesky-based reduced-rank square-root Kalman filtering, in: American Control Conference, 2008, pp. 3987–3992, IEEE, 2008.

de Leeuw, B., Dubinkina, S., Frank, J., Steyer, A., Tu, X., and Van Vleck, E.: Projected Shadowing-based Data Assimilation, arXiv preprint arXiv:1707.09264, 2017.

Frank, J. and Zhuk, S.: A detectability criterion and data assimilation for non-linear differential equations, arXiv preprint arXiv:1711.05039, 2017.

González-Tokman, C. and Hunt, B.: Ensemble data assimilation for hyperbolic systems, *Physica D: Nonlinear Phenomena*, 243, 128–142, 2013.

Grudzien, C., Carrass, A., and Bocquet, M.: Asymptotic forecast uncertainty and the unstable subspace in the presence of additive model error, arXiv preprint arXiv:1707.08334, 2017.

Gurumoorthy, K., Grudzien, C., Apte, A., Carrass, A., and Jones, C.: Rank deficiency of Kalman error covariance matrices in linear time-varying system with deterministic evolution, *SIAM Journal on Control and Optimization*, 55, 741–759, 2017.

Hamill, T. M. and Snyder, C.: A hybrid ensemble Kalman filter–3D variational analysis scheme, *Monthly Weather Review*, 128, 2905–2919, 2000.

Jazwinski, A. H.: Stochastic Processes and Filtering Theory, Academic Press, New-York, 1970.

Kalnay, E.: Atmospheric modeling, data assimilation and predictability, Cambridge University Press, 2003.

Kuptsov, P. and Parlitz, U.: Theory and Computation of Covariant Lyapunov Vectors, *Journal of Nonlinear Science*, 22, 727–762, 2012.



Legras, B. and Vautard, R.: A guide to Lyapunov vectors, in: ECMWF Workshop on Predictability, pp. 135–146, ECMWF, Reading, United Kingdom, 1996.

Lorenz, E. N. and Emanuel, K. A.: Optimal sites for supplementary weather observations: Simulation with a small model, *Journal of the Atmospheric Sciences*, 55, 399–414, 1998.

5 Nerger, L., Hiller, W., and Schröter, J.: A comparison of error subspace Kalman filters, *Tellus A*, 57, 715–735, 2005.

Ng, G., McLaughlin, D., Entekhabi, D., and Ahanin, A.: The role of model dynamics in ensemble Kalman filter performance for chaotic systems, *Tellus A*, 63, 958–977, 2011.

Palatella, L. and Trevisan, A.: Interaction of Lyapunov vectors in the formulation of the nonlinear extension of the Kalman filter, *Physical Review E*, 91, 042905, 2015.

10 Palatella, L., Carrassi, A., and Trevisan, A.: Lyapunov vectors and assimilation in the unstable subspace: theory and applications, *Journal of Physics A: Mathematical and Theoretical*, 46, 254020, 2013.

Penny, S. G.: Mathematical foundations of hybrid data assimilation from a synchronization perspective, *Chaos: An Interdisciplinary Journal of Nonlinear Science*, 27, 126801, 2017.

Pham, D., Verron, J., and Roubaud, M.: A singular evolutive extended Kalman filter for data assimilation in oceanography, *Journal of Marine Systems*, 16, 323–340, 1998.

15 Pires, C., Vautard, R., and Talagrand, O.: On extending the limits of variational assimilation in nonlinear chaotic systems, *Tellus A*, 48, 96–121, 1996.

Raanes, P., Carrassi, A., and Bertino, L.: Extending the square root method to account for additive forecast noise in ensemble methods, *Monthly Weather Review*, 143, 3857–3873, 2015.

20 Sakov, P. and Oke, P.: A deterministic formulation of the ensemble Kalman filter: an alternative to ensemble square root filters, *Tellus A*, 60, 361–371, 2008.

Shimada, I. and Nagashima, T.: A numerical approach to ergodic problem of dissipative dynamical systems, *Progress of Theoretical Physics*, 61, 1605–1616, 1979.

Trevisan, A. and Palatella, L.: Chaos and weather forecasting: the role of the unstable subspace in predictability and state estimation problems, *25 International Journal of Bifurcation and Chaos*, 21, 3389–3415, 2011a.

Trevisan, A. and Palatella, L.: On the Kalman Filter error covariance collapse into the unstable subspace, *Nonlinear Processes in Geophysics*, 18, 243–250, 2011b.

Trevisan, A. and Uboldi, F.: Assimilation of standard and targeted observations within the unstable subspace of the observation-analysis-forecast cycle, *Journal of the Atmospheric Sciences*, 61, 103–113, 2004.

30 Trevisan, A., D'Isidoro, M., and Talagrand, O.: Four-dimensional variational assimilation in the unstable subspace and the optimal subspace dimension, *Quarterly Journal of the Royal Meteorological Society*, 136, 487–496, 2010.

Vannitsem, S.: Predictability of large-scale atmospheric motions: Lyapunov exponents and error dynamics, *Chaos: An Interdisciplinary Journal of Nonlinear Science*, 27, 032101, 2017.

Whitaker, J. S. and Hamill, T. M.: Evaluating Methods to Account for System Errors in Ensemble Data Assimilation, *Monthly Weather Review*, 140, 3078–3089, 2012.



	Linear	weakly-nonlinear
<b>Perfect Model</b>	Filtering error covariances collapse to the span of the unstable-neutral BLVs and rank deficient filters, filtering only the $n_0$ leading BLVs, asymptotically equivalent to KF.	Ensemble based covariances project strongly onto the span of the leading $n_0$ BLVs when error growth is weakly-nonlinear. Inflation necessary due to sampling error when error growth is increasingly nonlinear.
<b>Additive Model Error</b>	True error covariance projects strongly onto the unstable, neutral and weakly stable BLVs. Dynamic upwelling transmits error from the unfiltered stable space to the filtered space, necessitating covariance inflation in the leading BLVs for rank deficient KF.	Inflation necessary in reduced rank extended and ensemble based Kalman filters to compensate for error growth in uncorrected modes, linear, dynamical upwelling on short time scales and sampling error from nonlinear error evolution on longer timescales.

**Table 1.** Summary of model scenarios and the need, and reasons, for covariance inflation in reduced rank Kalman filters.

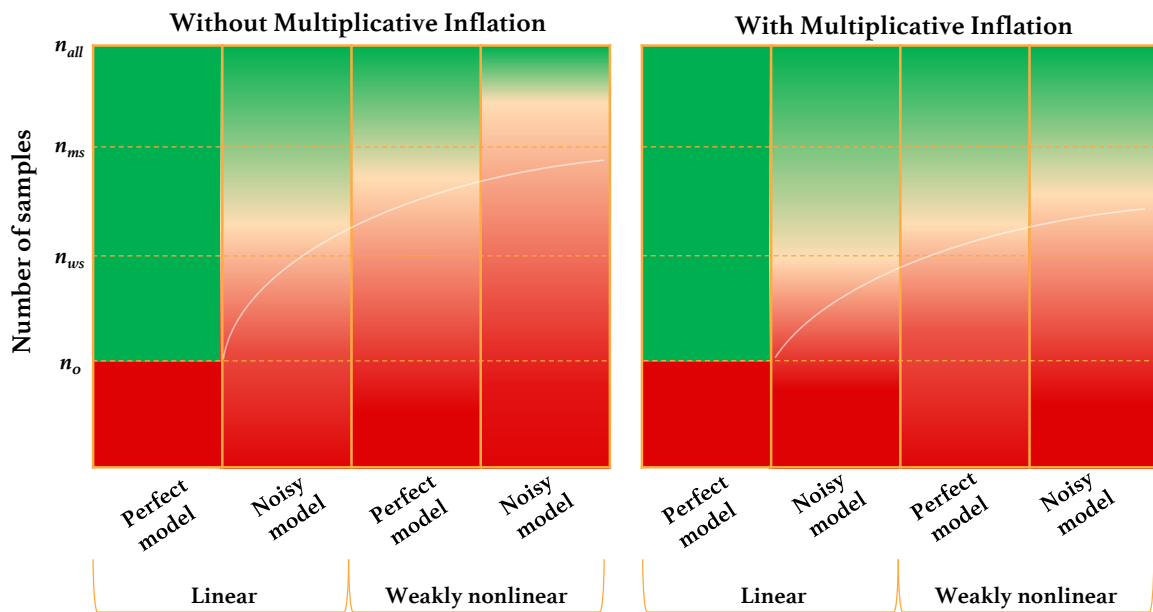


**Figure 5.** Conceptual representation of the number of samples necessary to prevent divergence of the EnKF in different filtering regimes. Dark green represents near-optimal filter performance and dark red represents filter divergence. In perfect-linear models, only  $n_0$  samples are needed for an asymptotically optimal performance. Without inflation, in noisy linear and perfect weakly-nonlinear regimes, near optimal performance can be obtained by correcting all modes up to the moderately stable BLVs — here  $n_{ws}$  corresponds to the number of unstable/ neutral/ weakly-stable modes, while  $n_{ms}$  furthermore includes moderately-stable modes. Additional samples may be necessary to control error growth with noisy, weakly-nonlinear evolution. Multiplicative inflation corrects for the upwelling from the uncorrected stable modes so that near optimal performance can be obtained when the error growth in unstable/ neutral/ weakly-stable modes are corrected.